



Correlative atom probe tomography and optical spectroscopy: An original gateway to materials science and nanoscale physics

Enrico Di Russo and Lorenzo Rigutti* 

Atom probe tomography (APT) correlated with optical spectroscopy has yielded original results in the domain of semiconductor nanoscale heterostructures. Statistical correlation (i.e., microscopy correlated with spectroscopy performed on macroscopic samples) has opened the way to a deeper understanding of carrier localization and recombination mechanisms in quantum-well systems. However, photoluminescence spectroscopy (PL) can be performed even on APT samples fabricated by focused ion beam, making it possible to perform sequential correlations on a single nanoscale object, which allows for a higher precision and accuracy. Finally, the laser pulse used for triggering the evaporation in laser-assisted APT can also generate a photoluminescence signal: this opportunity is exploited in the photonic atom probe. This instrument not only represents an original and effective way to perform *in situ* correlative microscopy, but also opens the way to study nanoscale physical phenomena driven by field, stress, or sample shape via the interpretation of the dynamically acquired APT and PL information.

Introduction

The use of ultrafast laser pulses, introduced since 2005, has opened up the possibility of the analysis of nonmetallic materials by atom probe tomography (APT),^{1,2} with important feedback in many fields of materials science^{3,4} and nanoscience,^{5–7} where it plays a key role in better understanding the link between composition and physical properties. At the same time, multi-technique, or correlative approaches^{8–12} have been recently developed. These allow not only to reach an ever more advanced level in the interpretation of the link between compositional, structural, and functional characteristics of materials, but also to achieve a deeper understanding of laser–matter interaction phenomena under high field. In this article, we will present the particular case where the APT is correlated with photoluminescence (PL) spectroscopy. Through this APT-PL approach, a wide class of functional materials can be studied in order to understand the relationship between the 3D distribution of the atomic constituents and optical properties. Among them we can mention the capability of absorbing or emitting light upon excitation and

how these responses depend on wavelength and polarization. These properties are crucial in the case of nanoscale systems constituting the building blocks of light-emitting or photovoltaic devices, but also of single photon sources for quantum cryptography. Objects such as quantum wells, quantum dots, nanoparticles embedded in insulating matrices, but also, in a crescendo of difficulty, extended or even point-like defects may be the object of such studies. Optical properties not only depend on the 3D distribution of the atomic species as it can be retrieved from APT data sets. Other structural factors, such as crystal symmetry or the degree of structural order, may also play a role, and a complete picture can be found in these cases through the complementary correlation of other techniques such as TEM. However, optical properties may also be influenced by environmental factors, such as temperature, presence of electric or strain fields, and by the specific morphology of the nanoscale system under study. This also opens the way to the study of the physics of APT in an original way, as the instrumental development of an atom probe capable of recording the PL signal during APT analysis demonstrates.¹³ We will

Enrico Di Russo, Department of Physics and Astronomy, Università degli Studi di Padova, Padua, Italy; enrico.dirusso@unipd.it

Lorenzo Rigutti, Normandie Université, UNIROUEN, INSA Rouen, CNRS, Groupe de Physique des Matériaux, Rouen, France; lorenzo.rigutti@univ-rouen.fr

*Corresponding author

doi:10.1557/s43577-022-00367-6

thus show how the relationship between optics and APT may on one hand disclose original opportunities in materials science, but on the other hand how it may reach far beyond this, toward a sort of nanoscale laboratory capable of generating new horizons of understanding and beauty.

Correlative methods with optical spectroscopy

A possible classification of correlative methods based on optical spectroscopy and APT follows.

Statistical correlation

This is the standard method applied to the interpretation of optical, chemical and morphological properties of nanoscale light emitters via APT. The optical properties are studied on a macroscopic portion of the sample, (e.g., a thin film or a large bunch of nanoscale objects). Micro-PL may allow for selecting a microscopic portion of the sample and extract its signal. The APT analysis is conducted on a nanometer-scale object extracted from the sample, without a strict relationship with the region probed by optical spectroscopy. A significant number of studies based on statistical correlation can be cited, for instance the studies on (In,Ga)N/GaN quantum wells performed by Oliver, Smith, Cerezo, Moody, and co-workers in Cambridge and Oxford. These works have assessed for instance the randomness of the In distribution within quantum wells grown on the polar c-plane of GaN and characterized the behavior of interfaces.^{14,15} These are important elements for the interpretation of the carrier localization mechanisms—and thus for the explanation of the radiative efficiency—within these quantum confined emitters that constitute the active region of standard LEDs.¹⁶ Other statistical

studies have pointed out that the (In,Ga)N behavior is different in quantum wells grown on nonpolar planes, on which In clustering becomes possible.^{17,18} However, there are many other examples of statistical correlation in the literature, not only on wide bandgap semiconductors,¹⁹ but also on semiconductor nanoparticles within insulating matrices^{20–22} and on III–V nanowires.²³

Sequential correlation on a single nanoscale object

In this advanced approach, illustrated within the scheme of **Figure 1a**, the optical and the APT analyses are carried out on the same individual nanoscale object. Intermediate TEM-micro-photoluminescence (μ PL) correlation is also possible and may add significant information, which is not accessible by APT only (e.g., crystal symmetries, presence of extended defects such as stacking faults or dislocations, etc.) or improve the information obtained by APT (e.g., by complementary electron tomography [ET]). However, we can mention only rare cases in which an individual sample survived three different types of analyses.^{10–24} It is crucial to note that sequential methods are based on the quite restrictive hypothesis that an APT sample is optically active. This requirement is far from obvious, as typical preparation methods require the use of focused ion beam (FIB), which introduces significant damage to the sample in terms of surface amorphization and swarms of point defects within up to several tens of nanometers from the surface. It is thus important that light emitters within APT samples are characterized by a strong localization of the carriers involved in the radiative transition: only in this way their wave functions avoid being influenced by the damaged regions close to the surfaces, which would otherwise yield an efficient

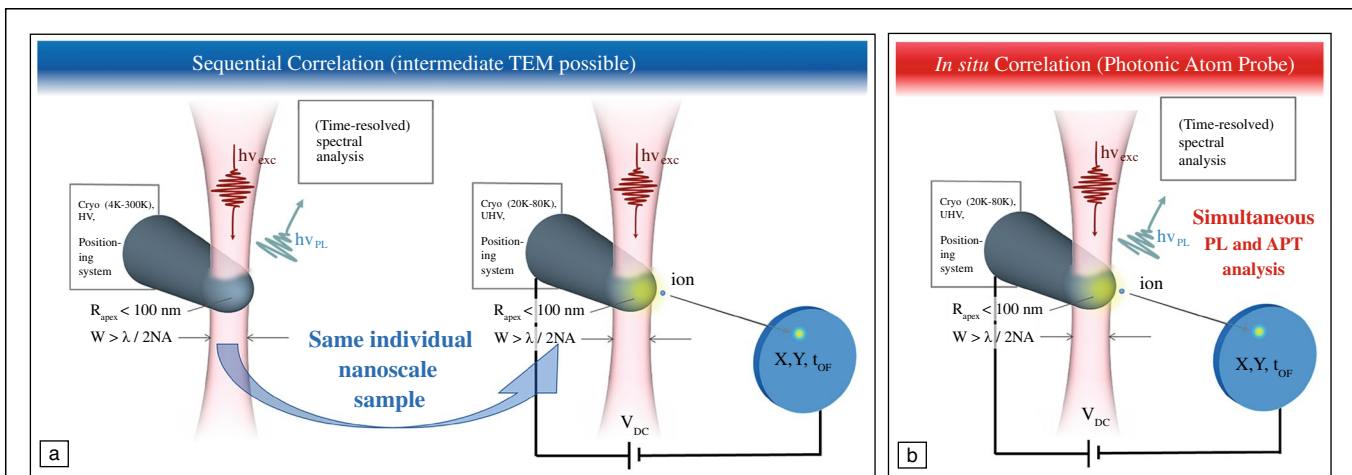


Figure 1. Advanced correlative methods based on photoluminescence spectroscopy and atom probe: (a) The sequential correlation is based on the analysis of a single individual nanoscale sample by micro-photoluminescence (μ PL) first, then by atom probe tomography (APT). An intermediate transmission electron microscopy (TEM) step is also possible, in order to access the structural properties otherwise not accessible by APT. (b) The *in situ* correlation has recently become possible thanks to the instrumental development of the photonic atom probe, in which PL spectroscopy may be carried out during APT analysis. Such methods allow for the interpretation of the optical properties of one or more individual nanoscale emitters on the base of APT data representing it or them in 3D.

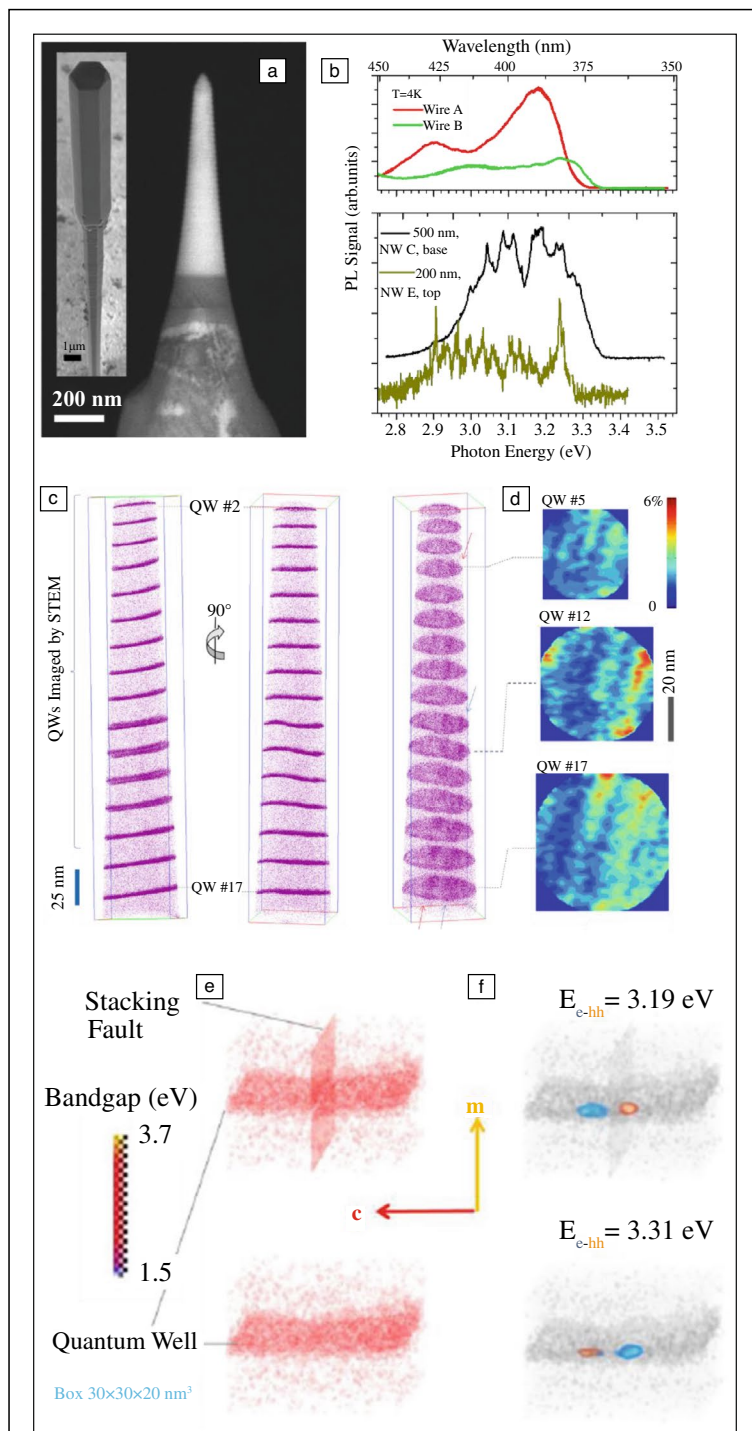


Figure 2. (a) Microwire (insert) and field-emission tip containing a set of (In,Ga)N/GaN quantum wells (QWs). (b) Micro-photoluminescence (μ PL) spectra issued from microwires (top), from a 500-nm-diameter cylinder fabricated by focused ion beam and from an atom probe tomography (APT) tip (bottom). (c) Three-dimensional reconstruction of the position of In atoms within the multi-QW system. (d) Composition maps from selected QWs. (e) Band-gap landscape. (f) Calculated electron-hole wave functions based on APT reconstructions with (top) and without (bottom) the effect of a stacking fault. Adapted with permission from Reference 10. © 2013 American Chemical Society and Reference 25. © 2016 American Institute of Physics.

source of nonradiative recombination paths. To date, III-N and II-O crystals have shown to be suitable for this approach.

In situ correlation via the photonic atom probe

The last type of correlation is achieved through a dedicated instrument that combines compositional/morphological analysis and optical spectroscopy capabilities, similar to what is implemented in the case of cathodoluminescence (CL) spectroscopy in an electron microscope (SEM or TEM). In the case of laser-assisted APT, it is a simple consideration that a laser pulse exciting a suitable sample at a proper wavelength and intensity can trigger ion evaporation in a tomographic atomic probe and, at the same time, excite electron-hole pairs that can recombine radiatively and generate a PL signal. An instrument exploiting both ionic and photonic signals has been recently developed at GPM in Rouen, and is referred to as the photonic atom probe,¹³ whose principle is schematically illustrated in Figure 1b. This instrument cannot only yield new performances in terms of correlative optical spectroscopy and atomic-scale microscopy, but also represent a new tool for the study of surface and bulk light-matter interaction phenomena at the nanoscale, with or without an intense applied electric field.

From a microwire to a nanotip

In order to correlate the 3D information provided by APT with the local PL signal, a bulk sample can be progressively milled by FIB until an optical active field-emission tip is formed.^{10,25} This process leads to substantial variations in the luminescence spectrum, reducing the emission intensity and gradually revealing more and more details of the PL fine structure.

This approach was successfully attempted to study the emission of a (In,Ga)N multi-quantum well (QW) system grown on the lateral and upper surface of GaN microwires (Figure 2a). The PL spectra of a microwire is represented in the top part of Figure 2b. Even if QWs typically present well-defined transition energies that are strictly linked to their morphology, composition, and homogeneity, the observed spectrum presents broad and continuous peaks in a wide spectral region between 2.9 and 3.3 eV. This suggests the presence of composition and/or morphology inhomogeneities in the QWs. Then, this spectrum was compared with those associated with a 500-nm-diameter nano-cylinder and with a \sim 100-nm-diameter needle-shaped APT tip containing only the upper part of the multi-QW system, that are represented in Figure 2b. Interestingly, discrete emission lines appear in the nano-cylinder PL spectrum. Similar lines are even better resolved

in the case of the nanotip, revealing the presence of several 5-meV large peaks that can be interpreted in terms of local carrier recombination within single QWs. Such a huge difference between the emission spectrum of the whole microwire and that associated with the resulting nanotip is due to the very little volume that is probed with the μ PL laser in the latter case.

The nanotip was then analyzed by APT. The 3D reconstruction depicted in Figure 2c shows the position of In atoms, revealing the QWs, but also the information of In-rich regions (Figure 2d) associated with the presence of planar stacking faults. Finally, the correlation between the structural and optical properties of the QWs was established through an effective mass calculation.¹⁰ The electron–hole wave functions (Figure 2f), as well as the transition energies, were calculated on the bandgap landscapes (Figure 2e) obtained on the basis of 3D chemical maps by including or neglecting the presence of In-rich stacking faults. Results are summarized in Figure 2f. The carrier localization in correspondence of the In-rich zones and of the stacking faults is also associated with a decrease in transition energies estimated to be about 15 meV. This result is in good agreement with the peak energy distribution observed in Figure 2b. Although it is not possible to strictly correlate each single QW with the relative emission line in the PL spectrum, this study confirms the possibility to statistically correlate the optical emission of a nanotip with its APT reconstruction.

The multimicroscopy approach

A more advanced statistical study was attempted performing a combination of sequential μ PL, ET, and APT on a set of several tens of samples.²⁴ The system designated for this study consists of a stack of GaN layers containing truncated hexagonal pyramidal quantum dots (QDs) arranged in columns. These structures are embedded in a matrix of AlN, acting as a barrier leading to the confinement of both electron and hole wave functions within the QDs. Because the confinement energy depends on both dimension and shape of the QDs, the 3D information provided by techniques such as APT or ET is crucial to predict the transition energy spectrum emitted by a specimen. In particular, ET is the ideal technique to determine the dimensions of 3D nano-objects embedded in a tip with subnanometer precision and it could also provide information to improve the accuracy of APT reconstructions. The 3D reconstruction of Ga atom positions provided by APT is illustrated in Figure 3a. Here, QDs appear as high-density Ga-rich regions with blurred outlines along the plane perpendicular to the tip evaporation direction, due to limitations of APT lateral resolution associated with low-range diffusion phenomena and local aberration effects. These problems are accentuated in correspondence of the GaN/AlN interfaces, due to the difference of the materials evaporation fields, as revealed by the composition map reported in Figure 3b. It should be noted that in this sample Ga/Al interdiffusion phenomena cannot occur during the growth process due to thermodynamic reasons. The vertical resolution of APT, in contrast, corresponds to an atomic monolayer (ML), that it is approximately equal to

about 0.25 nm. Three different approaches were then pursued in order to statistically correlate the QDs morphology with their recombination energy.

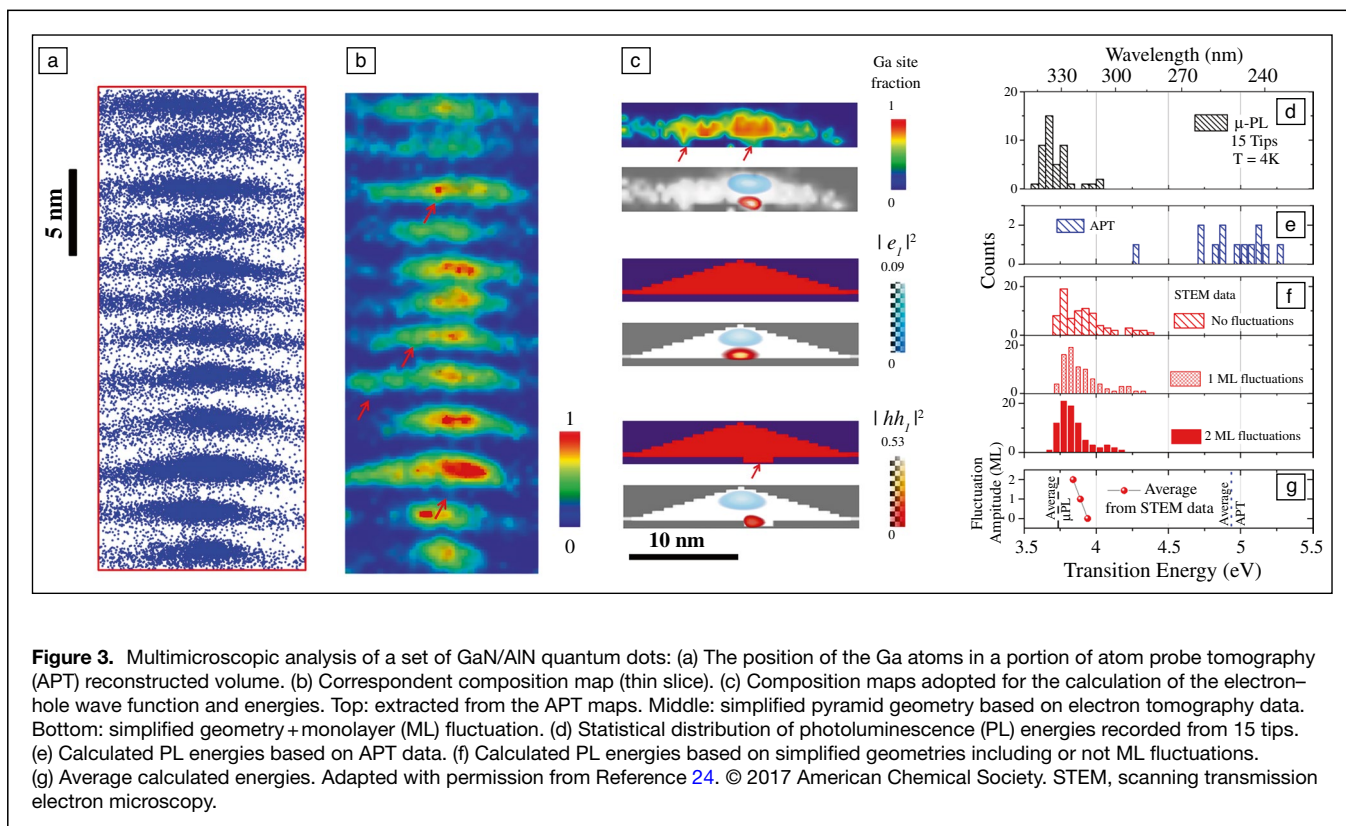
The 3D composition maps of the QDs extracted from the APT reconstruction may be interpreted as interface monolayer fluctuations at the bottom of the QDs, as indicated by the red arrows in Figure 3c (top). The formation of atomic steps on the barrier surface could be ascribed to the formation of extended defects (e.g., dislocations) that propagate through the heterostructure. However, it is also possible to describe the QDs through three parameters only as truncated pyramids, exploiting the data obtained by ET (Figure 3c, middle). This simple description may then be enriched by adding the bottom interface fluctuations suggested by APT. These fluctuations consist of either one or two monolayers, with 1.5-nm-diameter cylindrical shape (Figure 3c, bottom).

Comparing the emission spectra calculated based on APT data only (Figure 3e) with the experimental PL peak distribution (Figure 3d), the expected transition energies are overestimated. In fact, lateral resolution limitations of APT artificially leads to the mixture of Al and Ga in correspondence of the QDs lateral interfaces, increasing the material bandgap within QDs. Contrariwise, the transition energy distribution expected for pyramidal QDs is quite close to the emission energies observed in PL measurements, as displayed in Figure 3f, g. In addition, the introduction of interface fluctuations has the effects of localizing hole states (Figure 3c, bottom), lowering the average transition energy and providing a narrower energy distribution. Thus, the best statistical agreement with this experimental distribution is obtained considering pyramidal QDs with the geometrical parameters extracted from ET and bottom interfaces affected by monolayer fluctuations, as suggested by APT.

Photonic atom probe and super-resolution photoluminescence

The possibility of measuring PL spectra simultaneously with the APT analysis (i.e., during specimen evaporation) is the specific characteristic of the photonic atom probe. This opens up new methods and insights in the correlative analysis of optically active nanoscale systems. The PAP can be seen as the APT counterpart of cathodoluminescence in a scanning (transmission) electron microscope: it upgrades the instrument with optical spectroscopic capabilities, and it offers possibilities that go beyond the separated application of optical spectroscopy and structural/chemical/morphological study: as in many other systems, the whole is more than the sum of the parts. PAP has obviously very specific features. An example of this is discussed in the following.

The PAP analysis of a set of 5 ZnO QWs embedded inside a (Mg,Zn)O alloy grown on a ZnO substrate is synthetically displayed in Figure 4. These QWs have features that were particularly suitable for testing the new instrument: first, they have different thicknesses, which should result in different PL emission energies; second, they are quite closely packed with



each other, with a mutual distance of around 20 nm. The set of PL spectra acquired during the APT analysis is reported in Figure 4a. The series begins with the spectral index 1 and finishes with 53. Three main spectral regions may be identified as (1) the emission of the ZnO substrate, around 3.35 eV, (2) the emission of the QWs, between 3.35 and 3.55 eV, and (3) the emission from the (Mg,Zn)O alloy, which constitutes a band peaked at 3.67 eV. The basic concept for the interpretation of these data is that the signal originating from a given emitter disappears when the emitter is no longer there because it is evaporated. Disappearing spectral features are highlighted by the red arrows in the graph. This quite obvious state of things allows attributing the different spectral signatures to the different sample features that may be retrieved through the APT reconstruction. However, it is also possible to plot the PL data as differential spectra, as shown in Figure 4b. A differential spectrum being simply the difference between two consecutive spectra, this series of data emphasizes when main variations in the spectral intensity or energy occur. In this way, disappearing features in the PL series of spectra become peaks in the series of differential spectra. Such peaks (corresponding to the red arrows in Figure 4a) are marked within blue circles in Figure 4b.

The correlation of PL with APT may be straightforwardly carried out by analyzing the 3D reconstructions, in the form displayed in Figure 4c–d. As a guide for the reader, the position of the evaporation front during selected PL spectra acquisitions is underlined by red curves. The selected indices $i=7$,

11, 16, 24 correspond to the spectra in which the PL signals marked by the red arrows in Figure 4a disappear. It can be easily recognized that this sets an immediate correspondence between the disappeared spectrum and the QW that is about to be evaporated (as a matter of fact, QW PL signals have the tendency to disappear before the QW is completely evaporated, but this is expected because the structure of the QW is strongly affected even before its complete evaporation). Furthermore, differential spectra can be exploited in order to encode the intensities of different spectral intervals into the positions of the atoms, as displayed in Figure 4c. Here, it becomes immediately visible that the 3.42 eV signal (coded in green) is generated by QW5, while the 3.49 eV signal (in red) is generated from QW4.

In any case, the technique allows singling out the signal of an individual quantum confined system and to discriminate it among the neighboring emitters, which are as close as 20 nm. This spatial resolution (which is relative to the APT axis of analysis only) is over one order of magnitude smaller than the laser wavelength, which approximately corresponds to the standard spatial resolution of μ PL as set by the diffraction limit.

The PAP allows thus for super-resolution PL, which is a nice and (*a posteriori*) straightforward consequence of collecting a light signal from a slowly and gently evaporating tip. The cross-sectional composition map of Figure 4d exhibits quite clearly the alloy distribution, which can be studied by statistical means, and the presence of interface roughness. It

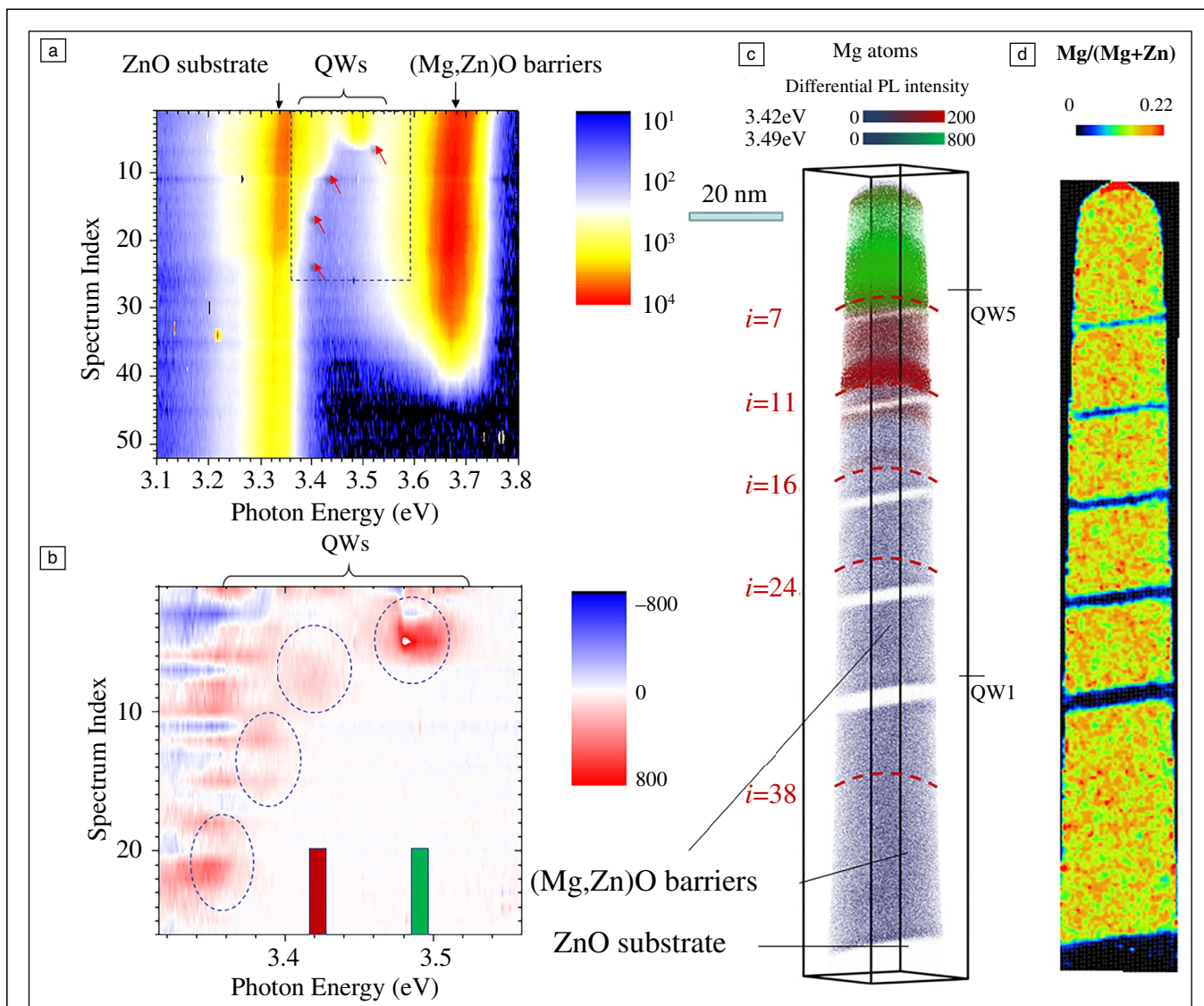


Figure 4. *In situ* photonic atom probe analysis of a system of 5 ZnO/(Mg,Zn)O quantum wells: (a) Complete set of collected micro-photoluminescence (μ PL) spectra, the red arrows indicating the approximate location of the disappearance of the PL peaks of consecutive quantum wells (QWs). (b) Differential spectra recorded in the sub-region indicated by the blue rectangle in (a). The optical signatures of four over five QWs are highlighted by the blue circles. (c) Three-dimensional reconstruction of the positions of Mg atoms; the color of the atoms is color-coded according to the PL intensities in the spectral intervals indicated at the top and in the graph in (b). The red dashed lines indicate the approximate position of the specimen surface during the acquisition of the i -th spectrum. (d) Two-dimensional distribution of the Mg II-site fraction calculated over a 5-nm-thick slice close to the tip axis. Adapted with permission from Reference 26. © 2020 American Chemical Society.

is well known that these features may be quite effective in the localization of carriers within the QW (especially of holes, localizing over the scale of only several nanometers). Such features are considered when calculations are performed in order to understand whether the behavior of the light emitter is expected within the most common models. For instance, we adopted the quite simplified but robust approach of conducting effective mass 6 bands calculations, and we found good agreement between the experimental PL energies and those calculated on the basis of the morphological and compositional characteristics of the system as obtained by APT.²⁶

These results demonstrate that the PAP can be profitably applied to materials science, in particular to the correlative study of optically active materials. Other studies have already been carried out in (In,Ga)N/GaN QD systems, and further studies are planned. Instrumental upgrades have already resulted in the possibility of longer and more reliable analyses, also benefiting from a larger field of view. In the meantime, it is necessary to explore its—still unknown—limits in terms of application to materials and systems (quantum emitters, extended or point defects, etc.). The main questions to be addressed are indeed the following: How many materials

systems under the form of an APT specimen may emit photoluminescence and how significant can be their study by this technique? The next few years will likely provide an answer to these questions.

A nanoscale laboratory for the study of light–matter–field interaction

Yet, the PAP being a microscope equipped with optical spectroscopy capabilities, its vocation reaches beyond the mere application to materials science studies. The PAP (as the APT itself, but differently) is also a nanoscale laboratory (i.e., it is possible to play with light, field, and matter to induce new or just so far unobserved phenomena taking place down to the nanometer level). One example of this is represented by the opto-mechanical studies of field-emission tips as a function of the applied field or of the evolution of their shape. Again, the PAP represents a quite original possibility of studying the optical properties of a nanoscale object, which changes its shape over time.

As it is known, the application of a high voltage to a tip results in stress building up at the apex. Many APT users are aware of that, especially when their sample fractures because it did not withstand mechanical stress. The relationship between field F and stress σ is quite simple, $\sigma = 1/2\epsilon_0 F^2$, which is by the way the same as in any metallic surface, including that of a planar capacitor. Due to the fact that even dielectric tips exhibit a metal-like apex surface under high field,²⁷ ϵ_0 is the vacuum permittivity, which is material-independent. Of course, we can wonder whether this formula also holds in the case of semiconducting tips. We know from past work that the electric field is supposed to be expelled from field-emission tips under high voltage,²⁷ but the measurement of stress in a nanoscale object is never an obvious experimental problem.

This problem was considered in the PAP experiment reported in **Figure 5**.²⁸ In this case, we analyzed a ZnO/(Mg,Zn)O double QW system, of which only one QW is optically active (in the APT reconstruction of **Figure 5a**, the optically active QW is the thinner one on the left, closer to the ZnO substrate). The series of PL spectra is shown in **Figure 5b**: the QW signal is clearly appearing emitting at an energy of around 3.45 eV, while the other two signals can be easily identified (see also **Figure 4**) as the emissions of the ZnO substrate and of the (Mg,Zn)O barrier. The PL energy of the QW gradually shifts over time. Its shift evolves with the progression of the evaporation, as shown in the right panel of the graph in **Figure 5d**. The left panel of the same graph also indicates a dependence on the application of the voltage before the evaporation. Quite clearly, this energy shift is related to the stress induced by the electric field. It is far from straightforward to evaluate the stress at the QW position, but it is fortunately possible. First, one has to understand how the apex stress is transmitted to the rest of the structure down the tip cone shaft—which can be performed once one knows the

morphology of the tip and the differences between the elastic constants of the materials composing the structure; then, from this stress the strain tensor can be retrieved (through the elastic constants). Finally, the strain tensor allows for the calculation of the bandgap shift via the set of deformation potentials. Two examples of calculations of locally resolved bandgap shifts are reproduced in **Figure 5c** for two different sample morphologies (i.e., at the evaporation beginning and close to the evaporation of the emitting QW). The bandgap shift represents per se a good estimation of the PL shift, which is reported in the graph of **Figure 5d**. As the apex stress was not a priori known, we let it span an interval within which the best fitting value of $\sigma = 1.25$ GPa could be found. This value corresponds to an apex average surface field $F = 16$ V/nm, which is consistent with the microscopic field evaluated through the charge state ratio statistics, $F_\mu = 20$ V/nm.

The whole picture is also consistent with the stress–field relationship, which is indirectly reported in the left panel of the graph: the PL shift exhibits indeed a quadratic dependence on the applied voltage. These results also confirm our past piezospectroscopic studies of color centers in diamond nanoneedles, which were performed in a proto-PAP not yet equipped with APT detectors.²⁹ They also provide an independent way of assessing surface electric fields, which play an important role in the field evaporation of compound materials.^{30,31}

Further phenomena are currently being studied. The data set of **Figure 5b** indicates that not only is there an energy shift, but also an intensity variation, which is far from obvious: Why does the QW PL intensity increase during the first phases of the evaporation? The mechanism leading to this intensity variation is possibly related to several factors: (1) the modification of the light emission pattern through the morphology variation, which could couple more or less radiation into the spectrometer; (2) the modification of charge generation, also related to the evolution of the absorption of light during evaporation; and (3) the evolution of the transport of charge carriers within the system—also related to the morphology change, to the stress or to the progressive erosion of regions with a high density of defects at the surfaces.

Perspectives

Currently, correlative APT and optical spectroscopy displays an intriguing set of possibilities that could be applied in materials science or in nanoscale physics. Even if in the opinion of the authors there is very little potential for its widespread application because of the complexity of the issued data sets, it may represent an original way to tackle specific materials science problems. For instance, the study of coupled QDs, the study of parametric dependences of spectral signatures on applied fields, all of this correlated with the sub-nanoscale resolution 3D distribution of atomic species. On the other hand, its nanoscale lab vocation discloses the possibility of new experiences targeting the transport of charge carriers in APT specimens, the

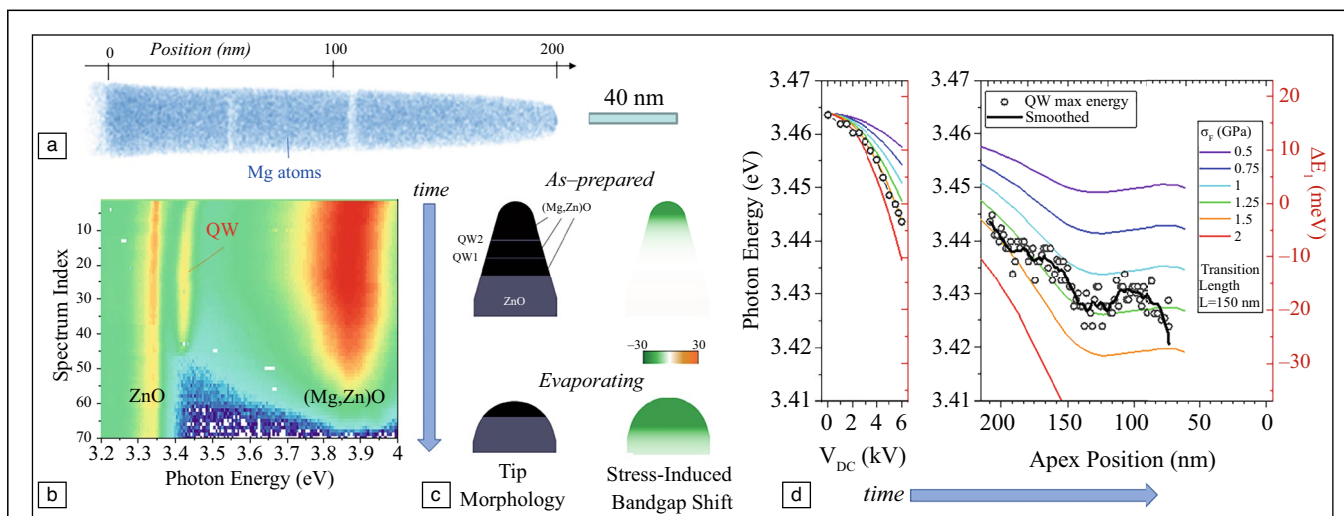


Figure 5. Study of stress-induced photoluminescence (PL) shift in a ZnO/(Mg,Zn)O QW within a photonic atom probe. (a) The reconstructed position of the Mg atoms. The emitting quantum well (QW) is the one at roughly 50 nm from the ZnO substrate/(Mg,Zn)O interface (set at 0). (b) Complete set of PL spectra acquired during the atom probe tomography acquisition. (c) Calculation of the distribution of the stress-induced bandgap shift within the tip at two different evaporation stages (beginning, top, and evaporation of QW1, bottom). (d) Comparison between the experimental and a set of calculated trends of the QW PL energy as a function of the applied voltage before evaporation (left panel) and as a function of the apex position during the evaporation. The best fitting curve is obtained for a stress at the apex equal to 1.25 GPa. Adapted with permission from Reference 28. © 2021 American Physical Society.

implementation of optically measured strain–stress curves. It may also allow for a deeper understanding of fracture events (they produce an electrical arc which could be recorded by the PL spectrometer) and of the chemical processes occurring at evaporating surfaces, with significant feedback for field-emission physics, APT metrology, and correlative microscopy.

Acknowledgments

The authors acknowledge funding from the French National Research Agency (ANR) in the framework of the projects EMC3 Labex AQUARATE, EMC3 Labex IDEPOP, and ANR-21-CE50-0016 ASCESE-3D, and co-funded in the framework of RIN IFROST, EMC3 Labex IDEPOP, and CPER BRIDGE projects by the European Union with the European Regional Development Fund (ERDF) and by Region Normandie.

Conflict of interest

No conflict of interests applies to this work.

References

1. L.J. Lauhon, P. Adusumilli, P. Ronsheim, P.L. Flaitz, D. Lawrence, *MRS Bull.* **34**(10), 738 (2009). <https://doi.org/10.1557/mrs2009.248>
2. A.D. Giddings, S. Koelling, Y. Shimizu, R. Estivill, K. Inoue, W. Vandervorst, W.K. Yeoh, *Scr. Mater.* **148**, 82 (2018). <https://doi.org/10.1016/j.scriptamat.2017.09.004>
3. A. Devaraj, R. Colby, W.P. Hess, D.E. Perea, S. Thevuthasan, *J. Phys. Chem. Lett.* **4**, 993 (2013). <https://doi.org/10.1021/jz400015h>
4. K. Stiller, L. Viskari, G. Sundell, F. Liu, M. Thuvander, H.-O. Andrén, D.J. Larson, T. Prosa, D. Reinhard, *Oxid. Met.* **79**, 227 (2013). <https://doi.org/10.1007/s11085-012-9330-6>
5. F. Letellier, L. Lechevallier, R. Lardé, J.-M. Le Breton, K. Akmalidov, S. Auffret, B. Dieny, V. Baltz, *J. Appl. Phys.* **116**, 203906 (2014). <https://doi.org/10.1063/1.4902954>

6. L. Amichi, I. Mouton, E. Di Russo, V. Boureau, F. Barbier, A. Dussaigne, A. Grenier, P.-H. Jouneau, C. Bougerol, D. Cooper, *J. Appl. Phys.* **127**, 065702 (2020). <https://doi.org/10.1063/1.5125188>
7. O.G. Licata, B. Mazumder, *Int. J. High Speed Electron. Syst.* **28**, 79 (2019). https://doi.org/10.1142/9789811216480_0005
8. A. Stoffers, J. Barthel, C.H. Liebscher, B. Gault, O. Cojocaru-Miréidin, C. Scheu, D. Raabe, *Microsc. Microanal.* **23**, 291 (2017). <https://doi.org/10.1017/S1431927617000034>
9. M. Herbig, D. Raabe, Y.J. Li, P. Choi, S. Zaefferer, S. Goto, *Phys. Rev. Lett.* **112**, 126103 (2014). <https://doi.org/10.1103/PhysRevLett.112.126103>
10. L. Rigutti, I. Blum, D. Shinde, D. Hernández-Maldonado, W. Lefebvre, J. Houard, F. Vurpillot, A. Vella, M. Tchermnycheva, C. Durand, J. Eymery, B. Deconihout, *Nano Lett.* **14**, 107 (2014). <https://doi.org/10.1021/nl4034768>
11. A. Stoffers, O. Cojocaru-Miréidin, W. Seifert, S. Zaefferer, S. Riepe, D. Raabe, *Prog. Photovolt. Res. Appl.* **23**, 1742 (2015). <https://doi.org/10.1002/pip.2614>
12. Z. Sun, O. Hazut, B.-C. Huang, Y.-P. Chiu, C.-S. Chang, R. Yerushalmi, L.J. Lauhon, D.N. Seidman, *Nano Lett.* **16**, 4490 (2016). <https://doi.org/10.1021/acs.nanolett.6b01693>
13. J. Houard, A. Normand, E. Di Russo, C. Bacchi, P. Dalapati, G. Beainy, S. Moldovan, G. Da Costa, F. Delaroche, C. Vaudolon, J.M. Chauveau, M. Hugues, D. Blavette, B. Deconihout, A. Vella, F. Vurpillot, L. Rigutti, *Rev. Sci. Instrum.* **91**, 083704 (2020). <https://doi.org/10.1063/5.0012359>
14. M.J. Galtrey, R.A. Oliver, M.J. Kappers, C.J. Humphreys, D.J. Stokes, P.H. Clifton, A. Cerezo, *Appl. Phys. Lett.* **90**, 061903 (2007). <https://doi.org/10.1063/1.2431573>
15. M.J. Galtrey, R.A. Oliver, M.J. Kappers, C. McAleese, D. Zhu, C.J. Humphreys, P.H. Clifton, D. Larson, A. Cerezo, *Appl. Phys. Lett.* **92**, 041904 (2008). <https://doi.org/10.1063/1.2829592>
16. C. Weisbuch, S. Nakamura, Y.-R. Wu, J.S. Speck, *Nanophotonics* **10**, 3 (2021). <https://doi.org/10.1515/nanoph-2020-0590>
17. F. Tang, T. Zhu, F. Oehler, W.Y. Fu, J.T. Griffiths, F.C.-P. Massabau, M.J. Kappers, T.L. Martin, P.A.J. Bagot, M.P. Moody, R.A. Oliver, *Appl. Phys. Lett.* **106**, 072104 (2015). <https://doi.org/10.1063/1.4909514>
18. F. Tang, T. Zhu, W.-Y. Fu, F. Oehler, S. Zhang, J.T. Griffiths, C. Humphreys, T.L. Martin, P.A.J. Bagot, M.P. Moody, S.K. Patra, S. Schulz, P. Dawson, S. Church, J. Jacobs, R.A. Oliver, *J. Appl. Phys.* **125**, 225704 (2019). <https://doi.org/10.1063/1.5097411>
19. N. Jeon, B. Loitsch, S. Morkoetter, G. Abstreiter, J. Finley, H.J. Krenner, G. Koblmuehler, L.J. Lauhon, *ACS Nano* **9**, 8335 (2015). <https://doi.org/10.1021/acs.nano.5b04070>
20. M. Roussel, E. Talbot, F. Gourbilleau, P. Pareige, *Nanoscale Res. Lett.* **6**, 164 (2011). <https://doi.org/10.1186/1556-276X-6-164>

21. G. Beainy, J. Weimmerskirch-Aubatin, M. Stoffel, M. Vergnat, H. Rinnert, C. Castro, P. Pareige, E. Talbot, *J. Appl. Phys.* **118**, 234308 (2015). <https://doi.org/10.1063/1.4938061>
22. G. Beainy, J. Weimmerskirch-Aubatin, M. Stoffel, M. Vergnat, H. Rinnert, P. Pareige, E. Talbot, *J. Phys. Chem. C* **121**, 12447 (2017). <https://doi.org/10.1021/acs.jpcc.7b03199>
23. L. Mancini, Y. Fontana, S. Conesa-Boj, I. Blum, F. Vurpillot, L. Francaviglia, E. Russo-Averchi, M. Heiss, J. Arbiol, A. Fontcuberta i Morral, L. Rigutti, *Appl. Phys. Lett.* **105**, 243106 (2014). <https://doi.org/10.1063/1.4904952>
24. L. Mancini, F. Moyon, D. Hernández-Maldonado, I. Blum, J. Houard, W. Lefebvre, F. Vurpillot, A. Das, E. Monroy, L. Rigutti, *Nano Lett.* **17**, 4261 (2017). <https://doi.org/10.1021/acs.nanolett.7b01189>
25. L. Mancini, D. Hernández-Maldonado, W. Lefebvre, J. Houard, I. Blum, F. Vurpillot, J. Eymery, C. Durand, M. Tchernycheva, L. Rigutti, *Appl. Phys. Lett.* **108**, 042102 (2016). <https://doi.org/10.1063/1.4940748>
26. E. Di Russo, P. Dalapati, J. Houard, L. Venturi, I. Blum, S. Moldovan, N. Le Biavan, D. Lefebvre, M. Hugues, J.M. Chauveau, D.C. Blavette, B. Deconihout, A. Vella, F. Vurpillot, L. Rigutti, *Nano Lett.* **20**, 8733 (2020). <https://doi.org/10.1021/acs.nanolett.0c03584>
27. E.P. Silaeva, L. Arnoldi, M.L. Karahka, B. Deconihout, A. Menand, H.J. Kreuzer, A. Vella, *Nano Lett.* **14**, 6066 (2014). <https://doi.org/10.1021/nl502715s>
28. P. Dalapati, G. Beainy, E. Di Russo, I. Blum, J. Houard, S. Moldovan, A. Vella, F. Vurpillot, N. Le Biavan, M. Hugues, J.M. Chauveau, L. Rigutti, *Phys. Rev. Appl.* **15**, 024014 (2021). <https://doi.org/10.1103/PhysRevApplied.15.024014>
29. L. Rigutti, L. Venturi, J. Houard, A. Normand, E.P. Silaeva, M. Borz, S.A. Malykhin, A.N. Obraztsov, A. Vella, *Nano Lett.* **17**, 7401 (2017). <https://doi.org/10.1021/acs.nanolett.7b03222>
30. L. Mancini, N. Amirifar, D. Shinde, I. Blum, M. Gilbert, A. Vella, F. Vurpillot, W. Lefebvre, R. Lardé, E. Talbot, P. Pareige, X. Portier, A. Ziani, C. Davesne, C. Durand, J. Eymery, R. Butté, J.-F. Carlin, N. Grandjean, L. Rigutti, *J. Phys. Chem. C* **118**, 24136 (2014). <https://doi.org/10.1021/jp5071264>
31. E. Di Russo, F. Moyon, N. Gogneau, L. Largeau, E. Giraud, J.-F. Carlin, N. Grandjean, J.M. Chauveau, M. Hugues, I. Blum, W. Lefebvre, F. Vurpillot, D. Blavette, L. Rigutti, *J. Phys. Chem. C* **122**, 16704 (2018). <https://doi.org/10.1021/acs.jpcc.8b03223> □



Enrico Di Russo received his PhD degree from the University of Rouen, France, in 2018. His research interests included the development of the “photonic atom probe” and the study of dissociation reactions occurring during atom probe tomography (APT). Afterward, he worked as a postdoctoral researcher at CEA-LETI, developing a unique expertise to study optoelectronic devices combining APT with other microscopy techniques such as electron holography and cathodoluminescence. In 2020, he moved toward the University of Padova to develop an innovative method to produce direct bandgap GeSn alloys by pulsed laser melting. Di Russo can be reached by email at enrico.dirusso@unipd.it.



Lorenzo Rigutti joined the instrumentation team at Groupe de Physique des Matériaux, Rouen, France, in 2012. He received his PhD degree from the University of Bologna, Italy (2006) and completed postdoctoral research at the Institute of Fundamental Electronics in Orsay, France. He is an expert in semiconductor physics and characterization. His current research focuses on compositional metrology by atom probe tomography (APT) and its correlation with optical spectroscopy. His recent studies have addressed individual APT specimens in sequence with micro-photoluminescence (μ PL), scanning transmission electron microscopy, and APT, demonstrating the possibility of measuring optical emission from field-emission tips within an APT instrument. He has also demonstrated the photonic atom probe, an instrument coupling APT and *in situ* μ PL. Rigutti can be reached by email at lorenzo.rigutti@univ-rouen.fr.